Madiedo *Earth, Planets and Space* 2014, **66**:70
http://www.earth-planets-space.com/content/66/1/70

Earth, Planets and Space
a SpringerOpen Journal

LETTER Open Access

Robotic systems for the determination of the composition of solar system materials by means of fireball spectroscopy

José M Madiedo[1,2]

Abstract

The operation of the automated CCD spectrographs deployed by the University of Huelva at different observatories along Spain is described. These devices are providing information about the chemical nature of meteoroids ablating in the atmosphere. In this way, relevant physico-chemical data are being obtained from the ground for materials coming from different bodies in the Solar System (mainly asteroids and comets). The spectrographs, which work in a fully autonomous way by means of software developed for this purpose, are being employed to perform a systematic fireball spectroscopic campaign since 2006. Some examples of meteor spectra obtained by these devices are also presented and discussed.

Keywords: Meteors; Meteoroids; Meteorites; Asteroids; Comets

Findings

Introduction

Meteoroids are solid particles with sizes ranging from several tens of microns to around 10 m. These are mostly originated from asteroids and comets, although the analysis of meteorites recovered on Earth show that some meteoroids can also come from other bodies, such as Mars and the Moon. The mechanisms that deliver these particles to Earth provide a unique opportunity to measure from the ground the physico-chemical properties of materials coming from different bodies in the Solar System, and this information could be employed to plan future space missions. These meteoroids are observed as meteors when they impact the Earth's atmosphere. Meteors can also be observed by seismic signals (e.g., Yamada and Mori 2012; Ishihara et al. 2012). Meteors with a luminosity higher stellar magnitude −4 are named fireballs. The light emitted by these phenomena during the ablation in the atmosphere of the progenitor meteoroid allows analyzing these events. Thus, when meteors are simultaneously detected from, at least, two different meteor stations, their atmospheric trajectory and radiant can be easily determined, and the orbit of the progenitor meteoroid in the Solar System can be calculated (Ceplecha 1987). Once the orbital parameters are known, the so-called dissimilarity criteria can be employed to infer which is the potential parent body of these particles (Southworth and Hawkins 1963; Drummond 1981; Jopek 1993; Valsecchi et al. 1999; Jenniskens 2008; Williams 2011; Madiedo et al. 2013a, 2014c).

On the other hand, a suitable technique to derive information about the chemical nature of meteoroids ablating in the atmosphere is meteor spectroscopy. Thus, the analysis of meteor spectra can provide useful information about the mechanisms that control the ablation process and about the chemical composition of meteoroids and meteor plasmas (Borovička 1993, 1994; Trigo-Rodríguez et al. 2003; Madiedo et al. 2013a, b). But, besides, this technique also provides information about the chemical nature of the parent body (asteroid or comet) of these meteoroids. Most of the signal in meteor spectra is related to the emission from neutral and singly ionized chemical elements. However, bands of different molecules (such as, for instance, CN, N_2, C_2, FeO, and CaO) have been also observed (Borovička 1994). With the aim to obtain and analyze these emission spectra, a network of automated CCD spectrographs has been

Correspondence: madiedo@cica.es
[1]Facultad de Ciencias Experimentales, Universidad de Huelva, Huelva 21071, Spain
[2]Departamento de Física Atómica, Molecular y Nuclear. Facultad de Física, Universidad de Sevilla, Sevilla 41012, Spain

setup in Spain. These are in operation since 2006 in the framework of the SPanish Meteor Network (SPMN). The University of Huelva is a pioneer in Spain in the development of these systems, and nowadays, this institution operates these devices from seven different observatories in this country (Table 1). These spectrographs have been configured as autonomous devices by means of software developed for this purpose. Additional software has been also developed to analyze the corresponding meteor spectra and the physical conditions in meteor plasmas. This research is being developed in the framework of a project named SMART, which is the acronym for Spectroscopy of Meteoroids in the Atmosphere with Robotic Technologies.

The first spectral devices setup in the framework of the SMART project, which were based on high-sensibility CCD video cameras endowed with holographic diffraction gratings, started operation in 2006 from the meteor observing station located at Sevilla and also at the mobile meteor observing station at Cerro Negro (station nos. 1 and 2 in Table 1, respectively). The first of these stations is performing since that year a systematic spectroscopic campaign. The latter, however, is setup when necessary in a dark countryside environment located at about 60 km north from Sevilla. From 2007 to 2010, four additional meteor-observing stations endowed with automated CCD video spectrographs were deployed (no. 3 to no. 6 in Table 1). The last one (La Pedriza) has been setup in Andalusia (south of Spain) by the end of 2013. The expansion of this network of spectral video devices has been favored by the deployment of new video meteor stations in Spain, which increased from 2 in 2006 to 25 in 2010. From 2011, however, additional efforts were made by setting up new automated spectrographs based on slow-scan high-resolution CCD devices. These also employ 1,000 lines/mm diffraction gratings and operate from station nos. 1 and 2 in Table 1 (Sevilla and Cerro Negro, respectively).

Favorable weather conditions in Spain play a key role in the successful development of the continuous spectroscopic campaign carried out within the SMART project. Thus, as a result of this survey several hundreds of meteor spectra have been recorded so far. These include emission spectra produced not only by sporadic fireballs but also by events associated to major and minor meteoroid streams. In this paper, a description of these systems is given and some relevant results are presented.

Instrumentation and data reduction techniques

The video spectrographs setup by the University of Huelva work in a fully autonomous way by means of the MetControl software, which is described below. This application has been developed in the framework of the SMART project. These spectrographs are slitless systems based on the same low-lux CCD video cameras employed at meteor stations in Table 1 to monitor meteor and fireball activity (Madiedo and Trigo-Rodríguez 2008). Thus, two different Watec cameras (902H2 and 902H2 Ultimate, manufactured by Watec Corporation, Tsuruoka-shi, Japan) are employed. A diffraction grating (500 or 1,000 lines/mm, depending on the device) is attached to the optics of each CCD video camera. These devices, which can image meteor spectra for events with a luminosity higher than mag. −3/−4, generate interlaced video imagery in AVI format by following the PAL video standard. Thus, the images are recorded with a resolution of 720 × 576 pixels at a rate of 25 frames per second (fps). So, their time resolution is of about 0.02 s (once the images are deinterlaced). This makes possible the analysis of the evolution with time of meteor spectra. Their typical spectral resolution is of about 2.5 nm/pixel. Each video spectrograph is connected to a PC computer by means of a video acquisition card (model DC60, manufactured by EasyCap Capture, Shenzhen, China). In this way, the images are stored on a hard disk, and no compression is employed in order to preserve image quality. The computers are synchronized by means of a GPS antenna (35-HVS, manufactured by Garmin, Schaffhausen, Switzerland) to keep a precise timing of meteor and fireball events. Since these video spectrographs are based on 8-bits (i.e., 256 gray levels) devices, the most intense emission lines can saturate the CCD sensor for very bright events. In fact, this is one of the major drawbacks of these devices. Despite the grating, these

Table 1 Geographical coordinates of the meteor observing stations involved in the recording of meteor spectra and devices employed (V: CCD video spectrographs, S: slow-scan CCD spectrographs)

Station no.	Station name	Longitude (W)	Latitude (N)	Alt. (m)	Devices
1	Sevilla	5° 58′ 50″	37° 20′ 46″	28	V + S
2	Cerro Negro	6° 19′ 35″	37° 40′ 19″	470	V + S
3	La Hita	3° 11′ 00″	39° 34′ 06″	674	V
4	Huelva	6° 56′ 11″	37° 15′ 10″	25	V
5	El Arenosillo	6° 43′ 58″	37° 06′ 16″	40	V
6	Sierra Nevada (OSN)	3° 23′ 05″	37° 03′ 51″	2896	V
7	La Pedriza (OAA)	3° 57′ 12″	37° 24′ 53″	1030	V

video spectrographs are sensitive enough to image mag. +2/+3 and brighter stars that can be employed for an astrometric analysis. Thus, atmospheric trajectories can also be calculated for multi-station events by following the planes intersection method (Ceplecha 1987) and, so, the evolution of the conditions in meteor plasmas as a function of height (and not just as a function of time) can be analyzed. These spectra are reduced by means of the CHIMET software, which was also developed in the framework of the SMART project and is described in (Madiedo et al. 2011).

On the other hand, the higher-resolution spectroscopes consist of five slitless slow-scan high-sensitivity CCD devices that employ 1,000 lines/mm diffraction gratings. Two of these are manufactured by ATIK (models ATIK 4000LE and ATIK 16HR, Norwich, England), and the other three are manufactured by SBIG (one ST10 and two ST8 CCD cameras, Santa Barbara, CA, USA). These operate since August 2011 from station nos. 1 and 2 in Table 1 (Sevilla and Cerro Negro, respectively), where an array of high-sensitivity CCD video cameras is also used for the monitoring of meteor activity. These spectrographs generate imagery in FITS files which are sent to GPS synchronized computers. The exposition time is adjusted according to the conditions of the night sky (typically, 30-s expositions are employed). These systems are currently covering an extension of about 50° × 50° in the night sky. Their typical spectral resolution is of about 0.8 nm/pixel. Dead time between images, which is of about 10 s, is one disadvantage with respect to the operation of CCD video spectrographs that can work continuously during the whole night. On the other hand, since no rotary shutter or any similar device is employed, these spectrographs are not useful to obtain meteor velocity data. Thus, they cannot be employed to obtain the orbit in the Solar System of the meteoroids producing the emission spectra. Nevertheless, their imagery can be combined with the recordings obtained by the CCD video devices to obtain such information.

The MetControl software

The MetControl software was initially developed to control the operation of remote meteor-observing stations at sites where human intervention was not always possible (Madiedo and Trigo-Rodriguez 2010). Later on, it was modified to achieve a fully automatic operation of the CCD video spectrographs employed in the framework of the SMART project. Nowadays, this application is being employed at the observing stations listed in Table 1. The software can work in client and server modes, as explained below.

Figure 1 shows a flow diagram of the MetControl software running in client mode. This is the mode corresponding to data acquisition. Under this configuration,

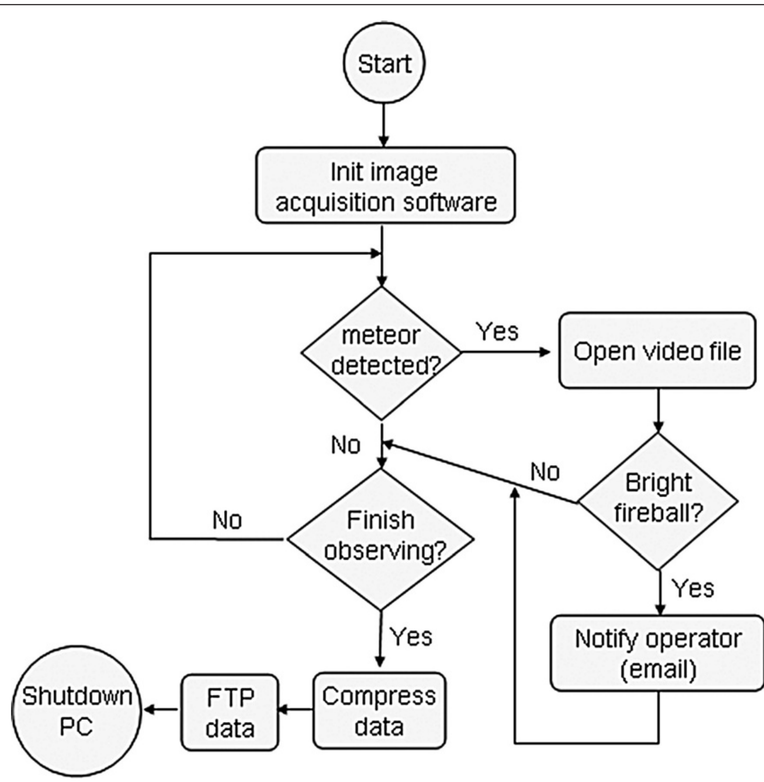

Figure 1 Flow diagram of the MetControl software running in client (or data acquisition) mode.

the application works as follows. First, by means of an appropriate BIOS configuration, the computers that are connected to the video spectrographs are configured so that they are automatically switched on when data acquisition must begin. Then, when a computer is switched on, the MetControl software is automatically started. The first task that this application performs is to start the data acquisition software, which monitors the night sky and stores a video file on the hard disk when a meteor is identified. During the observing session, MetControl checks periodically (typically every 30 s, although this interval can be modified by the user) if a new meteor trail has been recorded and the corresponding AVI video file has been stored on the hard disk. Every new AVI file is automatically opened by MetControl to check if an event brighter that mag. −3/−4 has been detected, since these can produce bright enough emission spectra to be recorded by the spectrographs. The software keeps a list of these events, and this list is emailed to the operator when the observing session is over. Besides, very bright fireballs (those with a luminosity above mag. −12) deserve special attention, since these events may give rise to meteorites. If such a bright event is detected, the software immediately sends an email to an operator together with an image of the bolide.

When the observing session is over, MetControl compresses the data recorded during the night and transfers them to a FTP server, where the information obtained by each device operating at the different stations is gathered and stored for further processing. In the event of power failure when data transfer is taking place, the computers are automatically started when power is restored, and then the transfer process is automatically resumed. When this data transfer to the FTP server is finished, the PC computers that control the spectrographs are switched off. This FTP server is located at station no. 1 in Table 1 (Sevilla). Another instance of MetControl running in server mode (or data processing mode) on this FTP server checks the incoming data (Figure 2). In this way, the software identifies which meteor trails have been simultaneously recorded from at least two different locations. The operator receives an automatic email notifying which meteor trails correspond to multi-station events. These can be reduced to obtain the atmospheric trajectory of the progenitor meteoroid, but also radiant and orbital information by employing the above mentioned techniques.

Emission spectra

Most of the meteor spectra recorded by the abovementioned spectrographs correspond to materials with chondritic composition (see, e.g., Trigo-Rodríguez et al. 2009; Madiedo et al. 2013a,b). But emission spectra produced during the ablation of achondritic meteoroids have also been imaged (Madiedo et al. 2014a). The video spectra produced by the three fireballs shown in Figure 3 are discussed below. These bolides were simultaneously recorded from, at least, two different meteor observing stations. In this way, their atmospheric trajectory could be calculated and the orbital elements of the progenitor meteoroids were also obtained (Tables 2 and 3). These data confirm that these events correspond to a Geminid

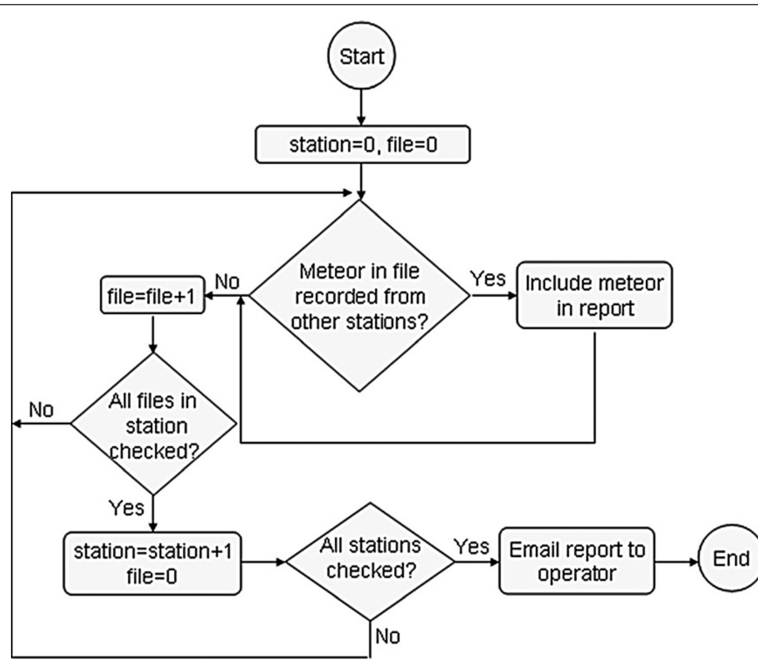

Figure 2 Flow diagram of the MetControl software running in server (or data processing) mode.

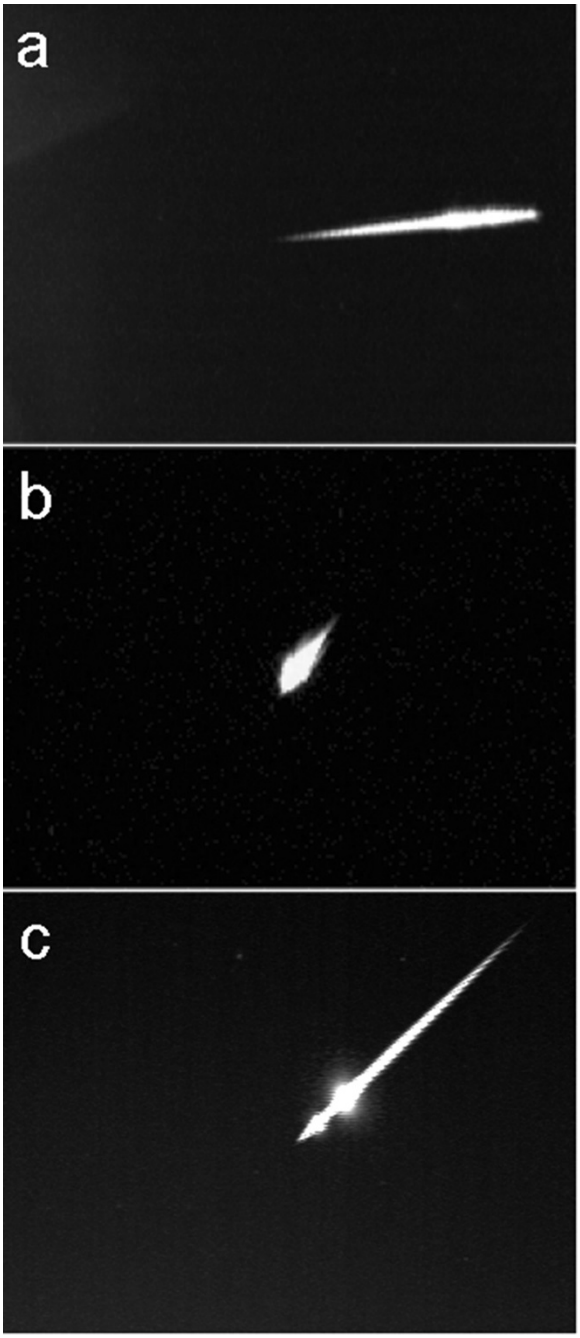

Figure 3 Composite image of the three fireballs whose emission spectra are discussed in the text. (a) SPMN151211 Geminid; **(b)** SPMN101212 Northern χ-Orionid; **(c)** SPMN270712 α-Capricornid.

bolide (Figure 3a), a Northern χ-Orionid (Figure 3b), and an α-Capricornid (Figure 3c) fireball, respectively. As an example, a composite image of the video spectrum recorded for the Geminid bolide is shown in Figure 4. The spectra of these fireballs were initially obtained as an intensity profile (pixel brightness, in arbitrary or device units, versus pixel number). This signal was then converted to intensity versus wavelength by identifying typical emission lines appearing in meteor spectra, such as the most prominent lines produced by chemical species such as Mg, Ca, and Na. This calibration in wavelength was performed by means of the CHIMET software (Madiedo et al. 2011). To accomplish this task, the program employs a database of frequencies at which typical emissions in meteor spectra appear. These frequencies have been taken from the NIST Atomic Spectra Database (http://physics.nist.gov/PhysRefData/ASD/lines_form.html). In this way, the software can overlap these theoretical emissions to the spectrum to be analyzed. When the user selects known lines in this spectrum, the software automatically fits the position of the theoretical emissions to these known lines. From this fit, an optimal overlap between theoretical and experimental emissions results and the calibration in wavelength of the experimental signal is obtained. Once this calibration is performed, the spectrum is corrected by taking into consideration the spectral response of the recording device. The response curve of the spectroscopic system is shown in Figure 3 in Madiedo et al. (2014a). In the following examples, multiplet numbers are given according to Moore (1945). It must be mentioned that ionized species such as, for instance, Mg II were not identified in these spectra and, so, the elemental abundances derived below correspond to neutral atoms.

The spectrum of a Geminid fireball

The parent body of the Geminid meteoroid stream is asteroid 3200 Phaeton. This produces the annual Geminid meteor shower, which is active from about November 27 to December 18 and peaks around December 14 (Jenniskens 2006). The perihelion distance of this stream is of about 0.14 AU, and this relatively small value has been correlated to the observed depletion of volatiles in Geminid meteoroids (Kasuga et al. 2006).

Figure 5 shows the emission spectrum produced by a mag. −5 Geminid fireball simultaneously recorded from station nos. 1 and 2 on December 15, 2011 at 1 h 22 m 24.2 ± 0.1 s UTC. The progenitor meteoroid impacted the atmosphere with an initial velocity of about 36.9 km s^{-1} (Table 2). This event was included in our database under the code SPMN151211, which was assigned after the recording date with format ddyymm. The most prominent emission lines have been highlighted in this plot. Most lines in the spectrum correspond to the emission from neutral Fe atoms, a situation which is common in meteor spectra (Borovička 1993, 1994). The most important contribution corresponds to Fe-23 (364.7 nm) in the ultraviolet. In this region of the spectrum, the H and K lines of Ca II (at 396.8 and 393.3 nm, respectively) can be also seen,

Table 2 Atmospheric trajectory and radiant data for the fireball discussed in the text (J2000)

Fireball	H_b (km)	H_e (km)	α_g (°)	δ_g (°)	V_∞ (km s^{-1})	V_g (km s^{-1})	V_h (km s^{-1})
SPMN151211 Geminid	94.2 ± 0.5	67.5 ± 0.5	115.8 ± 0.2	31.5 ± 0.2	36.9 ± 0.3	35.1 ± 0.3	33.5 ± 0.3
SPMN101212 N. χ-Orionid	95.1 ± 0.5	71.2 ± 0.5	81.1 ± 0.3	21.1 ± 0.2	26.6 ± 0.3	24.5 ± 0.3	37.9 ± 0.3
SPMN270712 α-Capricornid	99.7 ± 0.5	79.1 ± 0.5	300.7 ± 0.2	−9.9 ± 0.1	24.0 ± 0.3	21.5 ± 0.3	37.5 ± 0.3

α_g and δ_g denote the equatorial coordinates of the geocentric radiant. H_b, beginning height; H_e, ending height; V_∞, the initial (preatmospheric) velocity of the meteoroid; V_g, the geocentric velocity of the meteoroid; V_h, heliocentric velocity of the meteoroid.

although these are not individually resolved. The emission lines of Na I-1 (588.9 nm) and Mg I-2 (516.7 nm) are also very noticeable. The spectrum also contains atmospheric contributions, such as N_2 bands in the red region and the O I triplet at 777.4 nm.

An insight into the chemical nature of the progenitor meteoroid can be obtained by analyzing the relative intensity of the emission lines of multiplets Na I-1, Mg I-2, and Fe I-15 (Borovička et al. 2005). These relative intensities have provided the following intensity ratios: Na/Mg = 0.78 and Fe/Mg = 1.05. According to figure five in Borovička et al. (2005), the Na/Mg intensity ratio is in good agreement with the value expected for chondritic meteoroids moving at about 37 km s^{-1}. Besides, these relative intensities have been plotted on the ternary diagram shown in Figure 6, where the solid curve corresponds to the expected relative intensity for chondritic meteoroids as a function of meteor velocity (Borovička et al. 2005). This plot shows that, in fact, there is a good fit with respect to the expected value for chondritic materials. In addition, the averaged temperature of the meteor plasma and the relative abundances with respect to Fe for Na, Mg, and Ca have been estimated by following the technique described in (Borovička 1993). To derive these values, the intensity of the Na I, Mg I, Ca I, and Fe I lines highlighted in Figure 5 have been employed. The results are listed in Table 4, where the relative abundances inferred for other undifferentiated bodies in the Solar System have been also included (Jessberger et al. 1988; Rietmeijer & Nuth 2000; Rietmeijer 2002). These show that the abundances fit fairly well the expected value for chondritic materials with the exception of Ca, which is much lower than expected. Nevertheless, this can be explained on the basis of the incomplete evaporation of this element during ablation (Trigo-Rodríguez et al. 2003, 2009). The somewhat lower Na content, on the other hand, can be explained on the basis of the abovementioned relatively low perihelion distance of the Geminid stream (q = 0.14 AU), which results in depletion of volatiles in these meteoroids (Kasuga et al. 2006).

Spectrum of a Northern χ-Orionid fireball

The Northern χ-Orionid meteoroid stream produces an annual display of meteors from about December 1 to January 5, peaking around December 11 (Jenniskens 2006). The suggested progenitor body of this stream is the potentially hazardous asteroid (PHA) 2008XM1 (Madiedo et al. 2013a).

Figure 7 shows the calibrated emission spectrum of a mag. −6 Northern χ-Orionid fireball simultaneously recorded from station nos. 3 and 6 on December 2012, 10 at 5 h 42 m 50.7 ± 0.1 s UTC. According to Table 2, the meteoroid impacted the atmosphere with a velocity of ~26 km s^{-1}. This bolide received the code SPMN101212. The most significant contributions have been highlighted in this plot. Again, most lines correspond to Fe I. The spectrum is dominated by the contributions from Fe I-4 (385.8 nm) and Mg I-3 (382.9 nm), which appear blended in the signal, but also by the lines from Na I-1 (588.9 nm) and Mg I-2 (516.7 nm). The relative intensity of the emission lines of multiplets Na I-1, Mg I-2, and Fe I-15 are plotted in the ternary diagram in Figure 6, with Na/Mg = 0.85 and Fe/Mg = 0.86. This diagram shows that these intensities are in good agreement with respect to the value expected for chondritic meteoroids moving at a velocity of ~26 km s^{-1}. As can be noticed in Table 4, the relative abundances inferred from the analysis of the emission spectrum fit fairly well the values expected from chondritic materials. However, as in the case of the above-discussed Geminid fireball, the abundance of Ca is lower than expected as a consequence of the incomplete evaporation of this element during ablation.

Table 3 Orbital parameters (J2000) for the fireballs discussed in the text

Fireball	a (AU)	e	i (°)	ω (°)	Ω (°)
SPMN151211 Geminid	1.31 ± 0.02	0.907 ± 0.003	24.9 ± 0.6	327.5 ± 0.3	262.5421 ± 10^{-4}
SPMN101212 N. χ-Orionid	2.4 ± 0.1	0.79 ± 0.01	1.7 ± 0.2	95.44 ± 0.2	78.33956 ± 10^{-4}
SPMN270712 α-Capricornid	2.6 ± 0.1	0.76 ± 0.01	7.1 ± 0.1	262.8 ± 0.4	124.3210 ± 10^{-4}

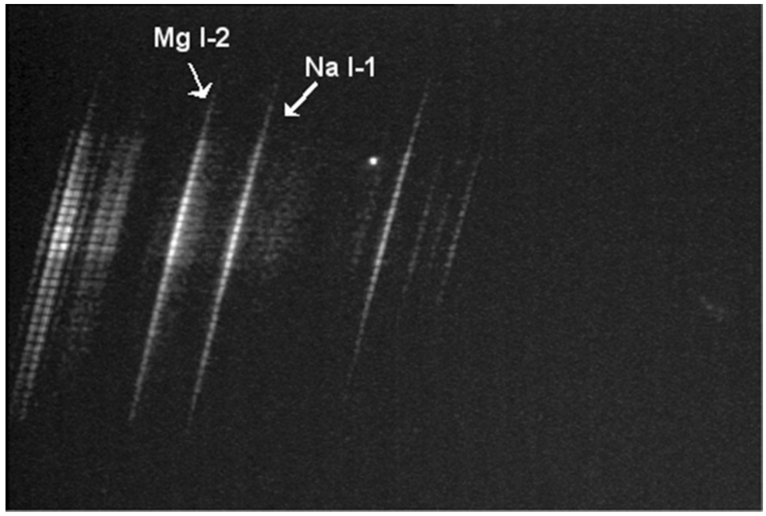

Figure 4 Composite image of the raw video spectrum imaged for the Geminid fireball discussed in the text.

Emission spectrum of an α-Capricornid bolide

The α-Capricornid meteor shower is active from about July 19 to August 18, with a maximum activity around the end of July (Jenniskens 2006). The Jupiter Family Comet 169P/NEAT (=2002EX12) has been recently identified as the parent body of this stream (Jenniskens & Vaubaillon 2010). Its perihelion distance ($q = 0.61$ AU) and short orbital period (about 4.2 years) suggest a rapid sublimation of volatiles from this cometary nucleus. However, recent observations of this object, with activity confined to the period around perihelion, indicate that 196P is a dying comet (Kasuga et al. 2010). Figure 8 shows the emission spectrum produced by a mag. −6 α-Capricornid fireball (code SPMN270712) recorded from station nos. 1, 4, 5, and 6 in Table 1 on July 27 2012, at 3 h 12 m 45.9 ± 0.1 s UTC. The progenitor meteoroid impacted the atmosphere with a velocity of around 24 km s^{-1}. Because of this relatively low velocity, the O I triplet at 777.4 nm was not detected, and the contribution from atmospheric N_2 bands in the red region is almost non-existent. With respect to meteoroid rock-forming elements, again, most lines are associated to neutral iron. The main contributions are those from Fe I-4 (385.8 nm) and Mg I-3 (382.9 nm), which appear blended in the ultraviolet, and the lines from Mg I-2 (516.7 nm) and Na I-1 (588.9 nm).

According to the measured relative intensities of lines corresponding to the Na I-1, Mg I-2, and Fe I-15

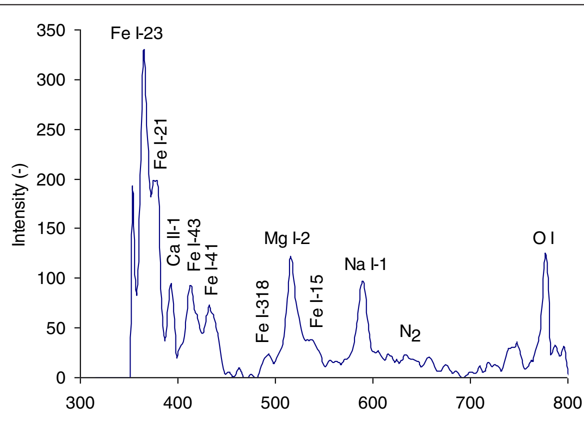

Figure 5 Calibrated emission spectrum of the Geminid fireball discussed in the text. Intensity is expressed in arbitrary units.

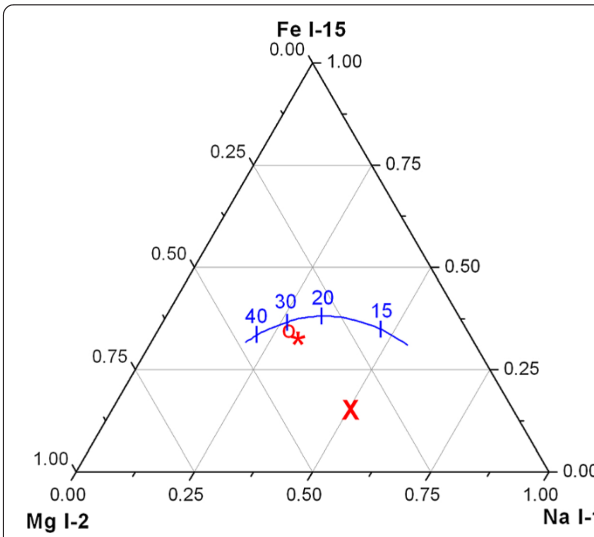

Figure 6 Expected relative intensity as function of meteor velocity (km s^{-1}) of Na I-1, Mg I-2, and Fe I-15 multiplets for chondritic meteoroids. Circle: SPMN151211 Geminid; asterisk: SPMN101212 Northern χ-Orionid; cross: SPMN270712 α-Capricornid fireball (Borovička et al., 2005).

Table 4 Elemental abundances relative to Fe derived for the fireballs analyzed in the text

Object	Mg	Na	Ca	*T* (K)
SPMN151211 Geminid	1.21	0.029	0.040	4400 ± 200
SPMN101212 N. χ-Orionid	1.06	0.040	0.029	4000 ± 200
SPMN270712 α-Capricornid	3.01	0.047	0.013	3600 ± 200
1P/Halley	1.93	0.193	0.121	-
IDPs	1.34	0.135	0.076	-
CI chondrites	1.17	0.066	0.078	-
CM chondrites	1.23	0.041	0.085	-

The abundances obtained for other Solar System undifferentiated materials are also indicated (Jessberger et al. 1988; Rietmeijer & Nuth 2000; Rietmeijer 2002).

multiplets, the Na/Mg and Fe/Mg intensity ratios yield 1.50 and 0.40, respectively. Once again, the Na/Mg intensity ratio fits the expected value for chondritic materials (figure five in Borovička et al. (2005)). However, the triangular diagram in Figure 6 shows that the meteoroid was Fe-poor, since the position corresponding to this particle falls well below the solid curve describing chondritic meteoroids at a velocity of around 24 km s^{-1}. This Fe depletion is confirmed by the relative abundances inferred from the emission spectrum and listed in Table 4. This table shows also that the meteoroid was Mg-rich, since the elemental abundance for this element is higher by a factor of about 2.5 with respect to the chondritic value. This is in agreement with the result obtained from the α-Capricornid spectrum analyzed by Borovička and Weber (1996). It is worth noting that a higher than chondritic Mg/Fe ratio was also found by Abe et al. (2005) when analyzing the emission spectrum of a bright Leonid fireball, produced by a meteoroid associated with comet 55P/Temple-Tuttle. One possibility for the Mg

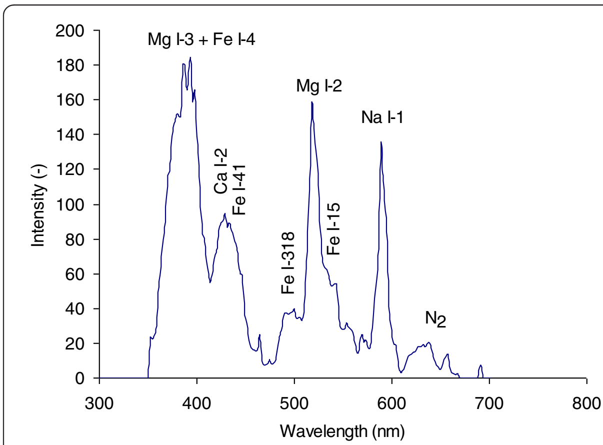

Figure 7 Calibrated emission spectrum of the Northern χ-Orionid fireball discussed in the text. Intensity is expressed in arbitrary units.

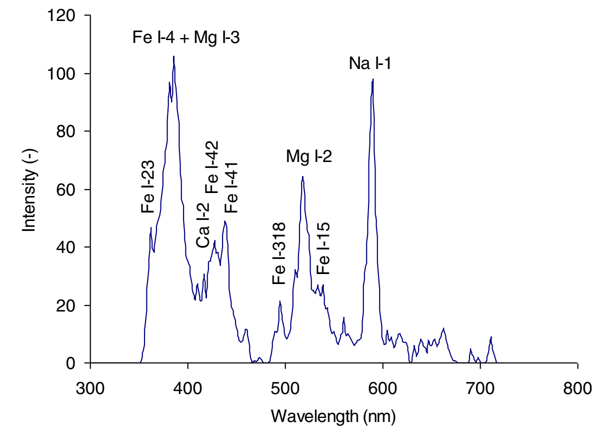

Figure 8 Calibrated emission spectrum of the α-Capricornid fireball analyzed in the text. Intensity is expressed in arbitrary units.

enrichment obtained from the analysis of this α-Capricornid spectrum could be associated to a high content in the parent comet of this stream (and so also in α-Capricornid meteoroids) of Mg-rich pyroxene, as has also been reported for comet Hale Bopp (Wooden et al. 1999). However, lower Mg abundances have been found for other for α-Capricornid fireballs, which imply inhomogeneities in the composition of the parent comet at the cm-level (Madiedo et al. 2014b). Again, the low Ca abundance would be a consequence of the incomplete evaporation of this element during ablation.

Conclusions

The spectrographs deployed in Spain in the framework of the SMART project have been described, and three emission spectra produced by bright fireballs from both asteroidal and cometary origin have been presented and discussed. The main conclusions derived from this analysis are given below:

(1) A software package (MetControl) has been developed to achieve an automated operation of these spectrographs. The images obtained by these systems can be used to obtain an insight into the chemical nature of meteoroids producing meteor events with a brightness above mag. −3/−4. In this way, information about the composition of different Solar System materials can be obtained. This chemical information could be employed to plan future space missions.

(2) The spectra recorded by the spectrographs contain contributions from Fe, Ca, Mg, and Na. These spectra can be employed to infer the likely chondritic composition of meteoroids and their parent bodies from the analysis of the relative intensity of emission lines produced by Mg I-2, Na

I-1, and Fe I-15 multiplets. Besides, abundances with respect to Fe of Mg, Na, and Ca can be calculated. Atmospheric nitrogen and oxygen contributions also appear in these spectra.

(3) Meteoroids produced by 3200 Phaeton and 2008XM1 have abundances of Na, Mg, and Ca compatible with the expected for chondritic materials. The lower-than-expected Ca abundances can be explained on the basis of the incomplete evaporation of this element during the ablation of these meteoroids in the atmosphere.

(4) The analysis of the spectrum produced by an α-Capricornid fireball indicates that progenitor meteoroid was Fe-poor with respect to the chondritic value. In addition, this particle exhibited an overabundance of Mg with respect to the expected value for chondritic materials. This could be associated to a likely high content of Mg-rich pyroxene in comet 169P/NEAT, as has also been reported for comet Hale Bopp.

Competing interests
The author declares that he has no competing interests.

Acknowledgements
The SMART project has been funded by the author of this paper and partially supported by the Spanish Ministry of Science and Innovation (project AYA2009-13227). I also thank *AstroHita Foundation* for its support in the establishment and operation of the automated meteor observing station located at La Hita Astronomical Observatory (La Puebla de Almoradiel, Toledo, Spain).

Received: 31 December 2013 Accepted: 30 June 2014
Published: 15 July 2014

References
Abe S, Ebizuka N, Yano H, Watanabe J, Borovička J (2005) Detection of the N_2^+ first negative system in a bright Leonid fireball. Astrophys J 618:L141–L144
Borovička J (1993) A fireball spectrum analysis. A&A 279:627–645
Borovička J (1994) Line identifications in a fireball spectrum. Astron Astrophys Suppl 103:83–96
Borovička J, Weber M (1996) An alpha-capricornid meteor spectrum. J Int Meteor Org 24:30–32
Borovička J, Koten P, Spurny P, Boček J, Stork R (2005) A survey of meteor spectra and orbits: evidence for three populations of Na-free meteoroids. Icarus 174:15–30
Ceplecha Z (1987) Geometric, dynamic, orbital and photometric data on meteoroids from photographic fireball networks. Bull Astron Inst Cz 38:222–234
Drummond JD (1981) A test of comet and meteor shower associations. Icarus 45:545–553
Ishihara Y, Hiramatsu Y, Yamamoto M, Furumoto M, Fujita K (2012) Infrasound/ seismic observation of the Hayabusa reentry: observations and preliminary results. Earth, Planets Space 64:655–660. doi:10.5047/eps.2012.01.003
Jenniskens P (2006) Meteor showers and their parent comets. Cambridge UniversityPress, Cambridge
Jenniskens P, Vaubaillon J (2010) Minor planet 2002 EX_{12} (=169P/NEAT) and the alpha capricornid shower. AJ 139:1822–1830
Jenniskens P (2008) Meteoroid streams that trace to candidate dormant comets. Icarus 194:13–22
Jessberger EK, Christoforidis A, Kissel J (1988) Aspects of the major element composition of Halley's dust. Nature 332:691–695
Jopek TJ (1993) Remarks on the meteor orbital similarity D-criterion. Icarus 106:603
Kasuga T, Yamamoto T, Kimura H, Watanabe J (2006) Thermal desorption of Na in meteoroids. Dependence on perihelion distance of meteor showers. AA 453:L17–L20
Kasuga T, Balam DD, Wiegert PA (2010) Comet 169P/NEAT (=2002 EX_{12}): the parent body of the α-Capricornid meteoroid stream. AJ 140:1806–1813
Madiedo JM, Trigo-Rodríguez JM (2008) Multi-station video orbits of minor meteor showers. Earth Moon Planets 102:133–139
Madiedo JM, Trigo-Rodriguez JM (2010) On the development of robotic CCD video meteor observing stations in Spain. In: Abstracts of the 41st Lunar and Planetary Science Conference. The Woodlands, pp 1–5
Madiedo JM, Toscano FM, Trigo-Rodríguez JM (2011) Software tools for the analysis of video meteors emission spectra. In: Abstracts of the EPSC-DPS Joint Meeting 2011. Nantes, pp 2–7
Madiedo JM, Trigo-Rodríguez JM, Williams IP, Ortiz JL, Cabrera J (2013a) The Northern χ-Orionid meteoroid stream and possible association with the potentially hazardous asteroid 2008XM1. MNRAS 431:2464–2470
Madiedo JM, Trigo-Rodríguez JM, Konovalova N, Williams IP, Castro-Tirado AJ, Ortiz JL, Cabrera-Caño J (2013b) The 2011 October Draconids outburst - II. Meteoroid chemical abundances from fireball spectroscopy. MNRAS 433:571–580
Madiedo JM, Trigo-Rodríguez JM, Williams IP, Konovalova N, Ortiz JL, Castro-Tirado JA, Pastor S, de los Reyes JA (2014a) Near-Earth object 2012XJ112 as a source of bright bolides of achondritic nature. MNRAS 439:3704–3711
Madiedo JM, Trigo-Rodríguez JM, Ortiz JL, Castro-Tirado AJ, Cabrera-Caño J (2014b) Orbit and emission spectroscopy of α-Capricornid fireballs. Icarus. doi:10.1016/j.icarus.2014.06.005
Madiedo JM, Trigo-Rodríguez JM, Ortiz JL, Castro-Tirado AJ, Cabrera-Caño J (2014c) Bright fireballs associated with the potentially hazardous asteroid 2007lq19. MNRAS. in press
Moore CE (1945) A multiplet table of astrophysical interest. Contributions from the Princeton Observatory. 20:1–110
Rietmeijer F (2002) The earliest chemical dust evolution in the solar nebula. Chemie der Erde 62:1–45
Rietmeijer F, Nuth JA (2000) Collected extraterrestrial materials: constraints on meteor and fireball compositions. Earth Moon and Planets 82–83:325–350
Southworth RB, Hawkins GS (1963) Statistics of meteor streams. Smithson Contr Astrophys 7:261
Trigo-Rodríguez JM, Llorca J, Borovička J, Fabregat J (2003) Chemical abundances determined from meteor spectra: I Ratios of the main chemical elements. Meteorit Planet Sci 38:1283–1294
Trigo-Rodríguez JM, Madiedo JM, Williams IP, Castro-Tirado AJ (2009) The outburst of the κ-Cygnids in 2007: clues about the catastrophic break up of a comet to produce an Earth-crossing meteoroid stream. MNRAS 392:367–375
Valsecchi G, Jopek T, Froeschlé C (1999) Meteoroid stream identification: a new approach - I Theory. MNRAS 304:743–750
Williams IP (2011) The origin and evolution of meteor showers and meteoroid streams. AG 52:2.20–2.26
Wooden DH, Harker DE, Woodward CE, Butner HM, Koike C, Witteborn FC, McMurtry CW (1999) Silicate mineralogy of the dust in the inner coma of comet C/1995 01 (Hale-Bopp) pre- and postperihelion. ApJ 517:1034–1058
Yamada M, Mori J (2012) Trajectory of the August 7, 2010 Biwako fireball determined from seismic recordings. Earth, Planets Space 64:27–35, doi:10.5047/eps.2011.08.021

doi:10.1186/1880-5981-66-70
Cite this article as: Madiedo: **Robotic systems for the determination of the composition of solar system materials by means of fireball spectroscopy.** *Earth, Planets and Space* 2014 **66**:70.